Electroluminescence of OLED based IrQ(ppy)$_2$-5Cl organometallic compound: Theoretical considerations

S. POLOSAN*, I. C. CIOBOTARU
National Institute for Materials Physics, Bucharest-Magurele 077125, Romania

The electroluminescence and current density versus applied voltage were measured for the OLED cell structure which contain IrQ(ppy)$_2$-5Cl as emitting layer. Two parameters, emission quantum yield and charge transport behaviors, which influences the electroluminescence, were modeled mainly concerning the non-radiative rate constants, delocalization of the HOMO and LUMO states, internal reorganization energies and bandgap of IrQ(ppy)$_2$-5Cl. The non-radiative constant rates were determined using the three zero-field splitting substates responsible for the phosphorescence model and shows an increasing of these rates together with a strong interaction with the polystyrene matrix. Delocalization of the HOMO and LUMO states on the quinoline ligand, together with the small reorganization energies and bandgap lowering indicates good charge transport properties for the IrQ(ppy)$_2$-5Cl compound.

(Received September 27, 2013; accepted January 22, 2014)

Keywords: OLED, Electroluminescence, Charge transport, DFT

1. Introduction

The basic OLED cell structure is a stacking of thin organic layers, sandwiched between a transparent anode and metallic cathode. The structure of the organic layers and the choice of anode and cathode are designed to maximize the recombination process in the emissive layer, thus maximizing the light output from the OLED device [1, 2].

The electroluminescence process of these devices includes several known steps: firstly, the injection of the charge carriers into organometallic compound from the cathode and anode, respectively.

Then, the electrons and holes traverse through the transport layers for both types of charges. It is followed by the capture processes when the electron and hole are sufficiently closer to each other to form the bounded electron-hole pair into the emissive layer. This layer is a dispersed organometallic compound into a conductive polymer.

These bounded pairs (excitons) recombine and decay radiatively to generate a photon that transverse the layers to the anode and the glass to escape from the OLED device. The whole process is known as electroluminescence, roughly defined as the ratio of the escaped photons versus charge carrier injections. [3, 4]

As organometallic compound, we recently proposed a dual phosphorescent iridium complex, further called IrQ(ppy)$_2$-5Cl [5]. The red and green phosphorescent colors come from two different ligands, phenylpyridine and quinoline, respectively. The temperature dependence of these red and green phosphorescence could give important details concerning the radiative and non-radiative processes which influences the electroluminescence properties of the OLED's based on the IrQ(ppy)$_2$-5Cl [6].

The aim of this paper details some theoretical considerations concerning the electroluminescence efficiency in the OLED based IrQ(ppy)$_2$-5Cl organometallic compounds starting from the experimentally measurements of the luminance and current-voltage characteristics. Mainly, it consists on the determining of the non-radiative transition rates which influences the emitting photon flux when the IrQ(ppy)$_2$-5Cl compound is embedded in polystyrene matrix. Some considerations concerning the efficiency of the charge transport across the IrQ(ppy)$_2$-5Cl neat films are based on the Density Functional Theory implemented in the Gaussian 03W software.

For the non-radiative transition rates, we use a model of three substates 1, 2 and 3 for the emitting ^{3}MLCT (Metal-to-Ligand Charge Transfer) triplet states, where non-radiative one-phonon relaxation is undertaken. This model is applied for the temperature dependence of the green phosphorescence, coming from phenylpyridine ligands, while the red phosphorescence, coming from the quinoline ligand, is neglected due to the weakness and slow temperature dependence.

2. Experimental

2.1 Theoretical considerations

In the OLED devices, the emission of light from the emitting layer results from the recombination of the electric-field-injected electrons and holes, also called "recombination electroluminescence". The electroluminescence of the OLED cells is defined as the photon flux per unit area emitted and can be expressing as [7]:

$$\phi_{EL} = \varphi \cdot P_s \cdot \gamma \cdot n_e \cdot n_h \cdot d \quad (1)$$

where φ is the emission quantum yield and defined as the ratio between radiative rate constant k_R and the total rate k_R+K_N which include non-radiative rate constant :

$$\varphi = \frac{k_R}{k_R + K_N} \tag{2}$$

P_S- is defined as the probability in the recombination event for the singlet exited state.

For the organometallic compounds for which the electroluminescence is based on the electron-hole recombination, it was confirmed the formation of three times more triplet excited than singlet excited states. In this case P_S is 1/4 due to the spin statistics [8].

The electron-hole recombination process is characterized by the second-order rate constant γ. Among the recombination processes an important role is played by the Langevin-type processes which describe the recombination from the organic materials [9]. In this model, the mean free path for optical phonon emission is small compared with the recombination of charges r_c:

$$l_0 \le r_c = \frac{e^2}{4\pi\varepsilon_o\varepsilon_r k_B T} \tag{3}$$

and then the charge carriers are statistically independent of each other. The recombination between them is a random process and is kinetically a bimolecular process with:

$$\gamma \approx \frac{e(\mu_e + \mu_h)}{\varepsilon_o\varepsilon_r} \tag{4}$$

In this kinetic model, n_e and n_h are the arbitrary electrons and holes concentrations and d is the thickness of the emitting layer.

Generally, the OLED structure has the luminescent material in the middle, embedded in the conducting polymers. The mobility of the charge carriers can be extracted from the current-voltage curves in which the current is limited due to the space-charge accumulation. The current density is given by:

$$j = \frac{8}{9}\varepsilon\mu\frac{V^2}{d^3} \tag{5}$$

where ε -is the permittivity of the conducting polymer, μ -is the charge carrier mobility, d- is the thickness of the conducting polymer and V-is the applied voltage[10].

In this way, both the electroluminescence and current density in the conducting polymer are dependent by the motilities of the charge carriers. The charge carries mobility has not a constant value but is dependent on the distribution energy in the hopping sites, being an exponential function of the electric field [11]:

$$\mu = \mu_o[\exp(\alpha E^{1/2})] \tag{6}$$

where μ_o - is the low field mobility and α - is a constant for a given sample. In this model, the electric field assists electrons in overcoming potential barriers due to the energy differences between sites.

This fact reveals the exponential behaviors for the both electroluminescence and the current-voltage characteristics as we will see in the experimental section. Among these parameters, we will try to model two factors:

a) the emission quantum yields φ which is dependent by the non-ratiative rate constant

b) the charge carriers mobility is described by the charge transfer rate given by the Marcus theory [12]. This charge transfer rate is influenced, among other parameters, by the internal reorganization energy which is determined by the fast change of the molecular geometry when a charge is added or removed from an organometallic molecule.

2.2 Computational details

Molecular geometry of $IrQ(ppy)_2$-5Cl have been optimized using Kohn-Sharm density functional theory (DFT) and computational calculations with Gaussian 03W software. We used the B3LYP hybrid exchange correlation functional of Becke three-parameters theory and the basic sets, Los Alamos National Laboratory double polarized functions (LANL2DZ). Theoretical studies on the ground state and excited electronic states of $IrQ(ppy)_2$-5Cl have been carried out using time-dependent density functional theory (TD-DFT). For time-dependent (TD-DFT), an additionally Electron Core Potential (ECP) for Ir atom was used.

The reorganization energy for the electron and hole for the $IrQ(ppy)_2$-5Cl molecule were predicted from the single point energy.

The rate equations for the populations of the substates at time t and temperature T are computed with the Wolfram Mathematica 8.0.

2.3 Synthesis

Meridional type Ir-compound was synthesized by the reaction of diiridium complex tetrakis (2-phenyl-pyridyl)-μ-(dichloro)diiridium ($[(C^N)_2Ir\text{-}\mu\text{-}Cl]_2$) with substituted 8- hydroxyquinoline.

$[(C^N)_2Ir\text{-}\mu\text{-}Cl]_2$

The mixture of 2-phenylpyridine (ppy) (9.5 ml, 66mmol), 2-ethoxyethanol (50 ml) and iridium trichloride hydrate (2 g, 6.7 mmol) was heated at 150^{o}C and refluxed under a nitrogen atmosphere for 8h. The precipitate were cooled and washed with ethanol, followed by acetone, and then dried in vacuum to yield yellow solids in 88% yield.

(8-Hydroxyquinolinato) bis(2-phenylpyridyl)iridium

The mixture of 2-ethoxyethanol (100 ml), $[(C^N)_2Ir\text{-}\mu\text{-}Cl]_2$ (1 g, 0.93 mmol), 8-hydroxyquinoline (0.35 g, 2.41 mmol) and sodium carbonate (1 g) were heated to reflux under a nitrogen atmosphere for 8h. It was then cooled to room temperature, while 2-ethoxyethanol was distilled off. The crude product was purified by silica gel column

chromatograph eluted with dichloromethane. After crystallization from dichloromethane, chemical yield of the yellow powder is about 37% [13].

For the photoluminescence measurements, 5 wt.% of mer–IrQ(ppy)$_2$–5Cl was dispersed in polystyrene and deposited on the quartz substrate. The photoluminescence (PL) spectra were measured at various temperatures between 10 K and 300 K with a Spex Fluorolog-3 fluorophotometer.

2.4. Device fabrication

Indium-tin oxide (ITO)-coated glass with sheet resistance of <50 Ω/cm^2 was used as substrate. The substrate was pre-patterned by photolithography. Pre-treatment of ITO includes a routine chemical cleaning using detergent and alcohol in sequence, followed by oxygen plasma cleaning. Thermal evaporation of organic materials was carried out at a chamber pressure of 10^{-6} Torr. Typical devices were configured as ITO/PEDOT:PSS or NPB (40 nm)/Ir-compound (6%) doped in CBP (10 nm)/BCP(6 nm)/AlQ3 or TPBI (40 nm)/LiF (1 nm)/Al (150 nm), where PEDOT:PSS, NPB, CBP, BCP, Alq3 and TPBI are poly(3,4-ethylene- dioxythiophene): poly (styrene sulfonate), 4,4'-bis[N-(1-naphthyl),N-phenylamino] biphenyl, 4,4'-bis(carbazol-9-yl) biphenyl,2,9-dimethyl-4,7-diphenyl-1,10-phenanthro -line, tris(8-hydoxyquinolinato) aluminium, and 2,2',2"-(1,3,5-benzenetriyl) tris-(1-phenyl-1H-benzimidazole), respectively.

For the devices using PEDOT:PSS, an aqueous solution was spin-coated onto the ITO plate at 4000 rps for 60 s to form a thin film, which was baked under vacuum at 120 ºC for 3 hr for dryness. Iridium complexes were co-evaporated with CBP to form films in ca. 6% wt ratio. After deposition of the electron-transporting layer, a thin film of LiF was followed. The devices were then capped with a thick layer of aluminum, which was served as cathode. Current voltage and light intensity measurements were done on a Source meter Keithley 2400 and a spectroradiometer Minolta Konica CS 2000A, respectively. All measurements were completed under ambient conditions.

2.5. Three zero-field splitting substates responsible for the phosphorescence

The rate equations for the populations $N_j(t)$ (j=1,2,3) of the substates at time t and temperature T are given by (7):

$$\frac{dN_4(t)}{dt} = -(k_4 + k_{41})N_4(t) + k_{14}N_1(t)$$

$$\frac{dN_3(t)}{dt} = -(k_3 + k_{32} + k_{31})N_3(t) + k_{23}N_2(t) + k_{13}N_1(t)$$

$$\frac{dN_2(t)}{dt} = k_{32}N_3(t) - (k_2 + k_{23} + k_{21})N_2(t) + k_{12}N_1(t)$$

$$\frac{dN_1(t)}{dt} = k_{41}N_4(t) + k_{31}N_3(t) + k_{21}N_2(t) - (k_1 + k_{12} + k_{13} + k_{14})N_1(t)$$

The emission intensity of Ir(ppy)$_2$-5Cl at time t is given by $I(t)*E_{photon}$ where E_{photon} is photon energy of luminescence and I(t) is given by:

$$I(t) = k_4N_4(t) + k_3N_3(t) + k_2N_2(t) + k_1N_1(t) \quad (8)$$

3. Results

The luminance and the current-voltage curves, in logarithmic scales, are presented in the Fig. 1. The luminance behaviors are dependent by the sandwich structure in which the IrQ(ppy)$_2$-5Cl compound is embedded. We have measured the luminance in two different sandwich structures in which we changed the Electron Transport Layer (ETL) from Alq_3 to TPBI.

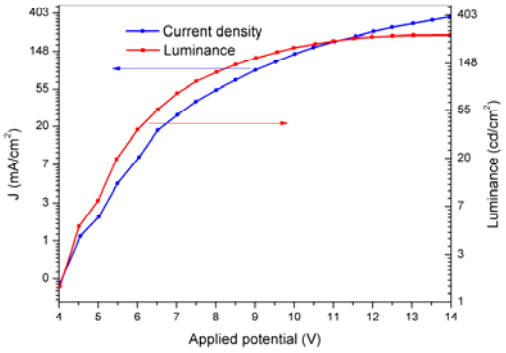

Fig. 1. Luminance and current density versus applied voltage for the IrQ(ppy)$_2$-5Cl embedded in CBP and using the Alq_3 as ETL (logarithmic scale).

In this figure, the luminance is given for the IrQ(ppy)$_2$-5Cl embedded in CBP and using the Alq_3 as ETL, because the luminance of this device is higher compared with the one with TPBI. The luminance is about 300 Cd/cm^2 and 450 mA/cm^2 at 14 V. The turn-on voltage is around 4 V. Compared with the photoluminescence measurement in which the green one is more intense than the red one, in the electroluminescence the red one is more intense and the green phosphorescence and appears only when we use Alq_3 as ETL. It is important to mention here the exponential behavior of the luminance up to 12 V and saturation over this value in our sandwich configuration.

The organometallic compounds are embedded in conducting polymers to avoid self-quenching of photoluminescence (PL) in neat films. Special organic host materials enhance the quantum efficiency by excitation transfer from host to the guest molecules.

The $Ir(ppy)_2$-5Cl is a dual emitter compound which exhibits two main phosphorescence colors: the green one, with three substates at 502 nm (2.47 eV), 531 nm (2.33 eV) and 565 nm (2.19 eV) and a red one at 667 nm (1.86 eV), all of them being triplet state emissions. The green phosphorescence comes from an emitting triplet state as consequence of the Metal-to-Charge Transfer of electrons from Ir to the pheylpiridine ligand.

Three zero-field splitting substates responsible for the phosphorescence model were applied for the most intense green emission from around 502 nm (2.47 eV) (Fig. 2). The temperature dependence of this phosphorescence has different behaviors compared with the green phosphorescence at 512 nm (2.42 eV) for $Ir(ppy)_3$ (Fig. 2, inlet). While the phosphorescence of the $Ir(ppy)_3$ has a maximum at around 180 K, the $IrQ(ppy)_2$-5Cl in polystyrene continuously decreases when the temperature increase, exceptions being a range of temperatures up to 10 K.

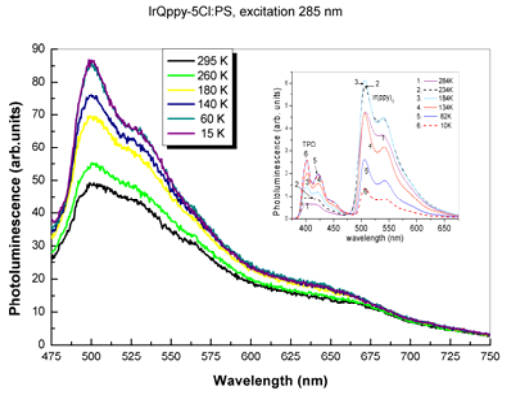

Fig. 2. Temperature dependence of the photo-luminescence for the IrQ(ppy)2-5Cl in comparison with the $Ir(ppy)_3$.

On a similar structure $Ir(ppy)_3$, Finkenzeller and Yersin have suggested that the emitting triplet state consists of three zero-field splitting substates 1, 2, 3 (Fig. 2, inlet) [14].

Theoretical studies of $Ir(ppy)_2$-5Cl bandgap have been carried out using density functional theory (DFT). There are several ^{3}MLCT triplet states located below the ^{1}MLCT singlet states for the phenylpyridine. When the $Ir(ppy)_2$-5Cl molecules are proper excited, the excitation is transferred from the metal-to-ligand charge transfer ^{1}MLCT singlet state to the ^{3}MLCT triplet states by internal conversion and intersystem crossing, for each type of ligand (Fig. 3).

Two lowest triplet states at 2.51 eV and 2.52 eV and another one at 2.6 eV comes from phenylpyridine ligands above the 1.85 eV triplet state from quinoline ligand. The two lowest triplet states are separated by 81 cm^{-1}. Therefore it is suggested that a relaxation process is undertaken between the relaxed 2.51 eV state and the nearby 2.52 eV state, but a smaller interaction with the 2.6 eV state at 300 K appears because of the wide gap between them.

For triplet emitting systems exist two kinds of energy transfers: one forms an endothermic energy transfer system where the T_1 level of the host is lower than the T_1 level of the guest. In the other form an exothermic system where the T_1 level of the host is higher than the T_1 level of the guest [15-17].

The study of the influence of host on emission of the phosphorescent materials gives important information on the development of phosphorescent OLEDs.

The lowest triplet state of polystyrene (PS) is located at lower energy (0.08 eV) than that of $IrQ(ppy)_2$-5Cl as shown in Fig. 3 [18].

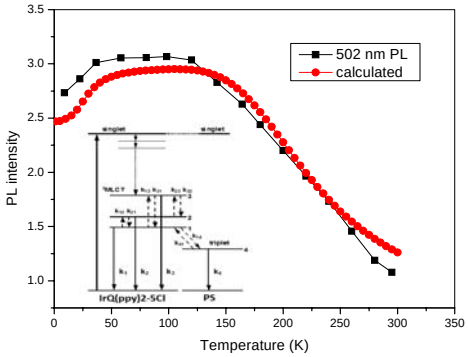

Fig. 3. PL intensity of $IrQ(ppy)_2$-5Cl doped in polystyrene experimentally measured (open circle) and theoretically calculated (solid line) at various temperatures. In the inlet, schematic energy level diagram of $IrQ(ppy)_2$-5Cl and PS with optical processes including one-phonon relaxation and the triplet-triplet annihilation.

Therefore $IrQ(ppy)_2$-5Cl doped in PS forms an endothermic system. The PL intensity of $IrQ(ppy)_2$-5Cl in PS increases with increasing temperature from 10 K to about 40 K. It is not clear whether the PL intensity does not change up to 120 K followed by slow temperature dependence.

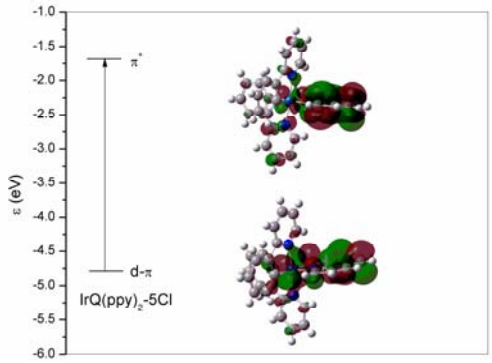

Fig. 4. The HOMO and LUMO bandgap and electron density distributions.

The bandgap of the IrQ(ppy)2-5Cl molecule, as a result of DFT calculation, was determined as 3.13 eV between the Highest Occupied Molecular Orbital (HOMO) and the Lowest Unoccupied Molecular Orbital (LUMO) states (figure 4).

The HOMO state has a lower metallic character at around 26%, which appear due to the hibridization between Ir *d*-orbitals and the π-orbitals of the quinoline ligand. [19].

Compared with the one for Ir(ppy)$_3$ which has a larger metallic characters of around 45% [20], the metal-to-ligand charge transfer in IrQ(ppy)$_2$-5Cl molecule significantly reduce the intensity of the red phosphorescence, which experimentally can be seen.

4. Discussions

The current-voltage curve follows a more general formula:

$$J = J_o(\exp(\alpha V^{1/2})]V^c \tag{9}$$

in which the material constant α is around 6 and *c*=13, suggesting a more complex dependence versus the applied voltage, but still an exponential mobility of the charge carriers.

We try to explain the observed temperature dependence of the PL intensity theoretically and quantitatively using a model of endothermic energy transfer from host PS to guest IrQ(ppy)$_2$-5Cl.

We assume that the energy transfer between the substate 1 and level 4 takes place by the non-radiative transitions through one phonon, i.e. (1) the phonon-assisted transition rate k_{41} from the level 4 to the substate 1 is given by $k_{41}=K_4 n$ (n is the occupancy of the effective phonon modes $n=[exp(E_{41}/kT)-1]^{-1}$).

Therefore we have to take into account the triplet-triplet annihilations from these levels of IrQ(ppy)$_2$-5Cl and PS. In the inlet of the Fig. 3 is shown only the case of the triplet-triplet annihilation, with annihilation rate k_{T1-PS}. We assume that $k_{T1\text{-}PS}$ consists of temperature-dependent term, i.e.

$$k_{14}=a+b[exp(-E_{14}/k_BT)] \tag{10}$$

where E_{14} is the thermal activation energy and *a* and b are the fitting parameters.

The radiative lifetimes of the substates 1, 2 and 3 have been estimated as 145, 11 and 0.75 μs, respectively. This indicates that the radiative transition rates k_1, k_2 and k_3 are given by $k_1=1/(145\times10^{-6})$ s^{-1}, $k_2=1/(11\times10^{-6})$ s^{-1}, $k_3=1/(0.75\times10^{-6})$ s^{-1}.

Regarding the coupling constant K_1 between the substates 1 and 2, K_2 between the substates 1 and 3, and K_3 between the substates 2 and 3, we use $K_2=K_3=1.1\text{x}10^6$ s^{-1} and $K_1= 0.005\text{x}10^6$ s^{-1}, which have been obtained from the fitting of the calculated photoluminescence (Fig. 3).

From the fitting procedure, we have determined the following parameters:

$$a=0.00808\text{x}10^6,\ E_{14}=0.08\ eV,\ b=3.5\text{x}10^8$$

The small value of the non-radiative constant K_1 which mainly influences the emission from the low lying triplet substate together with slow temperature dependence of the 502 nm (2.47 eV) photoluminescence when the IrQ(ppy)$_2$-5Cl is embedded in polystyrene, supports the idea of a strong interaction with the polystyrene matrix.

The non-radiative rate constant $1/K_1$=200 μs compete with the radiative rate constant of the low lying triplet substate from which we have the long lived phosphorescence.

Thus, the electroluminescence of IrQ(ppy)$_2$-5Cl compound embedded in polystyrene is reduced with around 50% only from the emission quantum yield besides the other factors of the charge carriers and the thickness of the emitting layer.

The HOMO state in IrQ(ppy)$_2$-5Cl molecule (4.84 eV) is almost the same in comparison with the one of Ir(ppy)$_3$ at 4.79 eV. The LUMO state in IrQ(ppy)$_2$-5Cl molecule (1.71 eV) (see Fig. 4) which comes from the quinoline ligand, is lowered compared with the one of the Ir(ppy)$_3$ at 1.22 eV. The decreasing of the bandgap has the consequence the lowering of the oxidation potential of the quinoline ligand compared with the phenylpyrydine ligand.

This fact is supported by the reorganization energy when one hole is captured in the HOMO state of the IrQ(ppy)$_2$-5Cl molecule. For these types of organometallic compound, Yershin developed a simple model in which the hole is firstly captured and forms an oxidized complex [8].

This process induces reorganization of the charged molecule modifying intramolecular distances, electronic energies, interactions with the host molecules, etc.

The calculated hole reorganization energy λ_h for the IrQ(ppy)$_2$-5Cl molecule is 0.22 eV, much lower compared with 0.242 eV for the mer-Alq$_3$ [21]. Similar value of 0.201 was obtained for the IrQ(ppy)$_2$. For the electron reorganization energy, the calculated value was 0.17 eV, slightly higher than 0.163 eV obtained for the IrQ(ppy)$_2$ but much lower than the one 0.276 eV for the mer-Alq$_3$ [22].

Because the electron reorganization energy is smaller compared with the mer-Alq$_3$, which is known as a good electron transport layer, the electron transfer rates may be higher in the IrQ(ppy)$_2$-5Cl molecule.

The charge transport properties can be connected with the spatial distribution of HOMO and LUMO states. Generally, a large delocalization of the HOMO and LUMO states ensure a better overlap between intermolecular orbitals and, therefore, a better electron/hole transport properties [23]. In the case of IrQ(ppy)$_2$-5Cl molecule, the HOMO and LUMO states are delocalized on the quinoline ligand.

This fact corroborated with the reorganization energies, smaller than for the mer-Alq$_3$ indicates that the IrQ(ppy)$_2$-5Cl is a good transport carriers. As a result, the electroluminescence of the OLED having IrQ(ppy)$_2$-5Cl

compound as emitting layer increases compared with the mer-Alq_3.

6. Conclusions

The efficiency of the electroluminescence process of the OLED structures with the $IrQ(ppy)_2$-5Cl compound as emitting layer are strongly influences by two parameters: the emission quantum yield and the charge carriers mobility, which can be theoretically computed.

For the case of $IrQ(ppy)_2$-5Cl compound embedded in polystyrene matrix, the higher non-radiative rate, attributed to the triplet-triplet annihilation between $IrQ(ppy)_2$-5Cl and PS, drastically reduce the emission quantum yield.

Moreover, the decreasing of the bandgap (compared with $Ir(ppy)_3$) leads to lowering of the oxidation potential of the quinoline ligand compared with the phenylpyrydine ligand. However, the delocalization of the HOMO and LUMO states on the quinoline ligand, together the small values of the reorganization energies for the charge carriers (compared with the mer-Alq_3) indicates good charge transport properties for the $IrQ(ppy)_2$-5Cl compound.

Acknowledgements

This work was supported by a grant of the Romanian National Authority for Scientific Research, CNCS-UEFISCDI, project number PN-II-ID-PCE-2011-3-0620. The work has been funded by the Sectorial Operational Program Human Resources Development 2007–2013 of the Romanian Ministry of Labor, Family and Social Protection through the Financial Agreement POSDRU/107/1.5/S/ 76903.

References

[1] Y. Kawamura, J. Brooks, J. J. Brown, H. Sasabe, C. Adachi, Phys. Rev. Lett., **96**, 017404 (2006).
[2] J. D. Slinker, A. A. Gorodetsky, M. S. Lowry, J. Wang, S. Parker, R. Rohl, S. Bernhard, G. G. Malliaras, J. Am. Chem. Soc., **126**, 2763 (2004).
[3] M. Eritt, C. May, K. Leo, M. Toerker, C. Radehaus, Thin Solid Films **518**, 3042 (2010).
[4] T. Tsuboi, J. Non- Cryst. Sol. **356**(37-40), 1919 (2010).
[5] T. Tsuboi, S. Polosan, D. F. Hang, T.J. Chow, Thin Solid Films **516**(9), 2788 (2008).
[6] S. Polosan, I. C. Radu, T. Tsuboi, J. Lum., **132**, 998 (2012).
[7] J. Kalinowski, J. Phys. D: Appl. Phys. **32**, R179 (1999).
[8] H. Yershin, W. J. Finkenzeller, WILEY-VCH Verlag GMBH&Co. KGaA, Weinheim, ISBN : 978-3-527-40594-7.
[9] M. Pope, C.E . Swenberg, Electronic processes in organic crystals, New York (1982).
[10] D. Ma, I. A. Hummelgen, X. Jing, Z. Hong, L. Wang, X. Zhao, F. Wang, J. Appl. Phys. **87**, 312 (2000).
[11] A. Ioannidis, E. Forsythe, Y. Gao, M. W. Wu, E. M. Conwell, Appl. Phys. Lett. **72**, 3038 (1998).
[12] R. A. Marcus, Rev. Mod. Phys. **65**, 599 (1993).
[13] D. F. Huang, T. J. Chow, C. Y. Wu, S. S. Sun, S.H. Tsai, Y. S. Wen, S. Polosan, T. Tsuboi, J. Chinese Chemical Soc. **55**(2), 439 (2008).
[14] W. J. Finkenzeller, H. Yershin, Chem. Phys. Lett., **377**, 299 (2003).
[15] M. A. Baldo, S. R. Forrest, Phys. Rev. B **62**, 10958 (2000).
[16] K. Goushi, R. Kwong, J. J. Brown, H. Sasabe, C. Adachi, J. Appl. Phys. **95**, 7798 (2004).
[17] M. A. Baldo, M. Segal, Phys. Stat. Solidi (a) **201**, 1205 (2004).
[18] S. Tagawa, N. Nakashima, K. Yoshihara, Macromolecules, **17**, 1167 (1984).
[19] S. Polosan, I. C. Radu, J. Nanoscience &Nanotechnology, **13**(7), 5203 (2012).
[20] P. J. Hay, J. Phys. Chem. A, **106**, 1634 (2002).
[21] L. L. Shi, Y. Geng, H. Z. Gao, Z. M. Su, Z. J. Wu, Dalton Trans., **39**, 7733 (2010).
[22] B. C. Lin, C. P. Cheng, Z. Q. You, C. P. Hsu, J. Am. Chem. Soc., **127**, 66 (2005).
[23] J. J. Kwiatkowsky, J. Nelson, H. Li, J. L. Bredas, W. Wenzel, C. Lennartz, Phys. Chem. Chem. Phys.**1852**, 10 (2008).

*Corresponding author: silv@infim.ro